QCD critical behavior in the PNJL model

Hubert Hansen [1]
Institut de Physique Nucléaire de Lyon, CNRS/IN2P3
Univ. Lyon 1, 69622 Villeurbanne Cedex, France

Abstract

In the first part of this paper, we will present a short introduction about the Nambu–Jona-Lasinio model coupled to the Polyakov loop. The aim of this effective model of QCD is to take into account features of both chiral symmetry breaking and deconfinement by using an effective potential fitted on lattice data obtained in the pure gauge sector. Results obtained for two light quark flavors in the mean field approximation at finite temperature and density will be discussed.

In the second part we will explore the phase diagram and critical behavior of this model with a focus on the isentropic lines.

1 The Polyakov – Nambu – Jona-Lasinio model

Confinement and chiral symmetry breaking are two of the most important features of quantum chromodynamics (QCD). Chiral models like the Nambu – Jona-Lasinio (NJL) model [1, 2] have been successful in explaining the dynamics of spontaneous breaking of chiral symmetry and its restoration at high temperatures and densities/chemical potentials. Recently, this and other types of models, together with an intense experimental activity, are underway to construct the phase diagram of QCD.

The NJL model describes interactions between constituent quarks, giving the correct chiral properties; static gluonic degrees of freedom are then introduced in the NJL Lagrangian through an effective gluon potential in terms of Polyakov loops [3, 4, 5] with the aim of taking into account features of both chiral symmetry breaking and deconfinement. The coupling of the quarks to the Polyakov loop leads to the reduction of the weight of the quarks degrees of freedom at low temperature, which is interpreted as a manifestation of confinement and is essential to reproduce lattice results. We emphasize that the reduction of the weight of the quark degrees of freedom might also have an important role for the critical behavior.

[1] In this paper I will shortly sketch results obtained in collaboration with P. Costa, M. Ruivo, C. Da Sousa, W. Alberico, A. Beraudo, M. Nardi, A. Molinari, C. Ratti.

$T = 0.26$ GeV$< T_0$
"Color confinement"
$\langle\Phi\rangle = 0 \longrightarrow$ No breaking of $\mathbb{Z}_3$

$T = 1$ GeV $> T_0$
"Color deconfinement"
$\langle\Phi\rangle \neq 0 \longrightarrow$ breaking of $\mathbb{Z}_3$

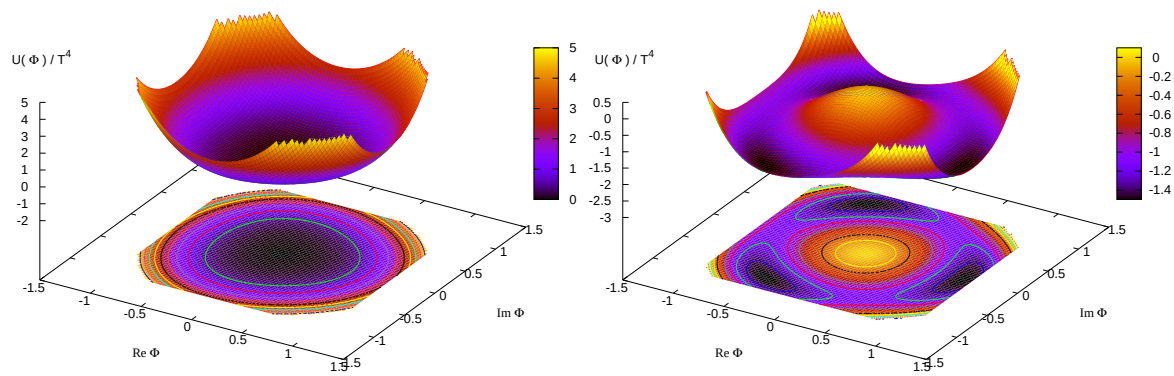

Figure 1: Effective potential in the pure gauge sector (Eq. (2)) for two characteristic temperatures, below and above the critical temperature T_0. One can see three minima appearing above T_0.

1.1 Pure gauge sector at finite temperature

Following the arguments given in [3] to study the $SU(N_c)$ phase structure, the appropriate order parameter (associated with $\mathbb{Z}_{N_c}$, center of $SU(N_c)$) is the Polyakov loop field:

$$\Phi(\vec{x}) \equiv \frac{1}{N_c}\,\mathrm{Tr}_c \left\langle\!\!\left\langle \mathcal{P}\exp\left[i\int_0^\beta d\tau\, A_4\left(\vec{x},\tau\right)\right] \right\rangle\!\!\right\rangle_\beta . \tag{1}$$

In the above, $A_4 = iA^0$ is the temporal component of the Euclidean gauge field $(\vec{A}, A_4)$, in which the strong coupling constant g_S has been absorbed, $\mathcal{P}$ denotes path ordering and the usual notation $\beta = 1/T$ has been introduced with the Boltzmann constant set to one ($k_B = 1$). An effective potential is built, respecting the symmetries of the original Lagrangian and conveniently chosen to reproduce results obtained in lattice calculations. In this approximation one simply sets the Polyakov loop field $\Phi(\vec{x})$ equal to its expectation value Φ =const., which minimizes the potential[2]:

$$\frac{\mathcal{U}\left(\Phi,\overline{\Phi};T\right)}{T^4} = -\frac{b_2\left(T\right)}{2}\overline{\Phi}\Phi - \frac{b_3}{6}\left(\Phi^3+\overline{\Phi}^3\right) + \frac{b_4}{4}\left(\overline{\Phi}\Phi\right)^2 , \tag{2}$$

[2]It exists other form for this potential [6].

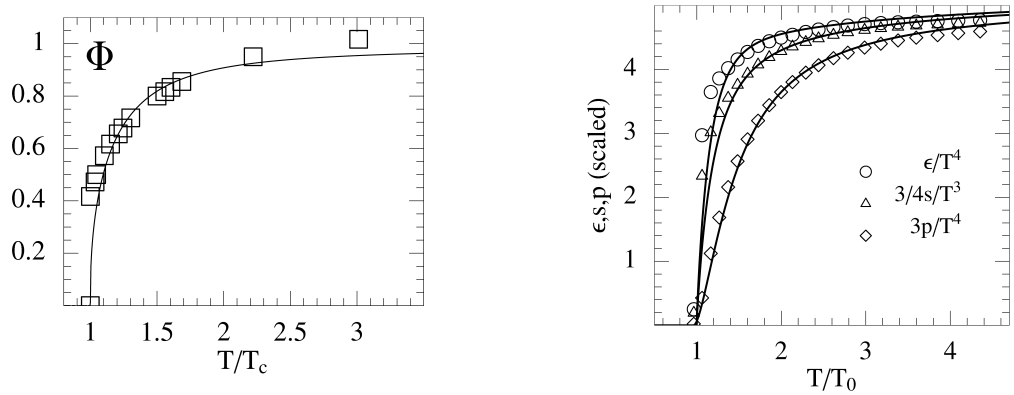

Figure 2: Comparison of pure gauge lattice results and calculation done with the potential $\mathcal{U}\left(\Phi,\overline{\Phi};T\right)$. Left panel: Polyakov loop (Lattice: O. Kaczmarek *et al*, Ref. [7]). Right panel: Scaled pressure, entropy and energy density (Lattice: G. Boyd *et al*, Ref. [7]). From Claudia Ratti *et al*, Ref. [4].

$$\text{where} \quad b_2\left(T\right) = a_0 + a_1\left(\frac{T_0}{T}\right) + a_2\left(\frac{T_0}{T}\right)^2 + a_3\left(\frac{T_0}{T}\right)^3. \tag{3}$$

$T_0 = 270$MeV is the critical temperature for the deconfinement phase transition according to pure gauge lattice findings[3].

The effective potential presents the feature of a phase transition from color confinement ($T < T_0$,the minimum of the effective potential being at $\Phi = 0$) to color deconfinement ($T > T_0$, the minima of the effective potential occurring at $\Phi \neq 0$) as it can be seen from Fig. 1. The potential possesses the $\mathbb{Z}_3$ symmetry but above T_0 it presents three minima, hence leading to a spontaneous symmetry breaking mechanism. A precision fit of the coefficients a_i, b_i has been performed in Ref. [4] to reproduce the expectation value of the Polyakov loop (Fig. 2, left panel): $a_0 = 6.75$, $a_1 = -1.95$, $a_2 = 2.625$, $a_3 = -7.44$, $b_3 = 0.75$, $b_4 = 7.5$. By minimizing this potential, one is able to compute a pressure, an entropy and an energy density in very good agreement with lattice findings (Fig. 2, right panel).

1.2 Coupling between quarks and the gauge sector

The Polyakov – Nambu – Jona-Lasinio (PNJL) model attempts to describe in a simple way the two characteristic phenomena of QCD, namely deconfinement and chiral symmetry breaking. In order to describe the coupling of light quarks to the chiral condensate $\langle\overline{q}q\rangle$ (order parameter of the chiral symmetry), we start from a two flavor NJL description of quarks (global $SU_c(3)$ symmetric and chirally invariant point-

[3]The range of applicability of our model is limited to temperatures $T \leq 2.5\ T_c$.

like interaction), coupled in a minimal way to the Polyakov loop via the following Lagrangian [4]:

$$\mathcal{L}_{PNJL} = \overline{q}\left(i\gamma_\mu D^\mu - \hat{m}_0\right)q + G_1\left[\left(\overline{q}q\right)^2 + \left(\overline{q}i\gamma_5\vec{\tau}q\right)^2\right] - \mathcal{U}\left(\Phi[A],\overline{\Phi}[A];T\right), \tag{4}$$

where $q = (q_u, q_d)$ are the quark fields and where the covariant derivative reads $D^\mu = \partial^\mu - iA^\mu$ with $A^\mu = g_S\mathcal{A}^\mu_a(x)\frac{\lambda_a}{2}\delta^\mu_0 A^0$ and $A^\mu = \delta^\mu_0 A^0$ (Polyakov gauge), with $A^0 = -iA_4$. The two-flavor current quark mass matrix is $\hat{m}_0 = diag(m_u, m_d)$ and we shall work in the isospin symmetric limit with $m_u = m_d \equiv m_0$; G_1 is the coupling strength of the chirally symmetric four-fermion interaction. Finally this model being non-renormalizable one also introduces a tridimensional ultraviolet cut-off Λ.

The parameters entering into the NJL part of Eq. (4) are $\Lambda = 651$ MeV, $G_1 = 5.04$ GeV^{-2} and $m_0 = 5.5$ MeV. They are fixed to reproduce the mass of the pion $m_\pi = 139.3$ MeV and its decay constant $f_\pi = 92.3$ MeV (obtained in a Hartree + Ring (RPA) calculation) as well as the chiral condensate at zero temperature and density $|\langle\overline{q}q\rangle|^{1/3} = 251$ MeV. The constituent (Hartree) quark mass is $m = 325$ MeV.

1.3 Results at finite temperature and density in the Hartree approximation

The usual techniques can be used to obtain the PNJL grand potential from the Hartree propagator[4]:

$$\begin{aligned}\Omega = \Omega(\Phi,\overline{\Phi},m;T,\mu) \;&=\; \mathcal{U}\left(\Phi,\overline{\Phi},T\right) + \frac{(m-m_0)^2}{4G_1} - 2N_cN_f\int_\Lambda \frac{\mathrm{d}^3p}{(2\pi)^3}\,E_p \\ &-2N_f\,T\int\frac{\mathrm{d}^3p}{(2\pi)^3}\left\{\mathrm{Tr}_c\ln\left[1+L^\dagger\mathrm{e}^{-(E_p-\mu)/T}\right] + \mathrm{Tr}_c\ln\left[1+L\mathrm{e}^{-(E_p+\mu)/T}\right]\right\}\,.\end{aligned} \tag{5}$$

In the above formula $E_p = \sqrt{\vec{p}^{\,2}+m^2}$ is the Hartree single quasi-particle energy (which includes the constituent quark mass). Besides for $N_c = 3$:

$$\mathrm{Tr}_c\ln\left[1+L^\dagger\mathrm{e}^{-(E_p-\mu)/T}\right] \;=\; \ln\left\{1+3\overline{\Phi}e^{-(E_p-\mu)/T}+3\Phi e^{-2(E_p-\mu)/T}+e^{-3(E_p-\mu)/T}\right\} \tag{6}$$

$$\mathrm{Tr}_c\ln\left[1+L\mathrm{e}^{-(E_p+\mu)/T}\right] \;=\; \ln\left\{1+3\Phi e^{-(E_p+\mu)/T}+3\overline{\Phi}e^{-2(E_p+\mu)/T}+e^{-3(E_p+\mu)/T}\right\} \tag{7}$$

The solutions of the mean field equations are obtained by minimizing the grand potential with respect to m, Φ and $\overline{\Phi}$, namely $\frac{\partial\Omega}{\partial\Phi} = 0$, $\frac{\partial\Omega}{\partial\overline{\Phi}} = 0$ and $\frac{\partial\Omega}{\partial m} = 0$. The latter coincides with the gap equation:

$$m - m_0 = 2G_1N_fN_c\int\frac{\mathrm{d}^3p}{(2\pi)^3}\frac{2m}{E_p}[\theta(\Lambda^2-p^2) - f^+_\Phi(E_p) - f^-_\Phi(E_p)]\,. \tag{8}$$

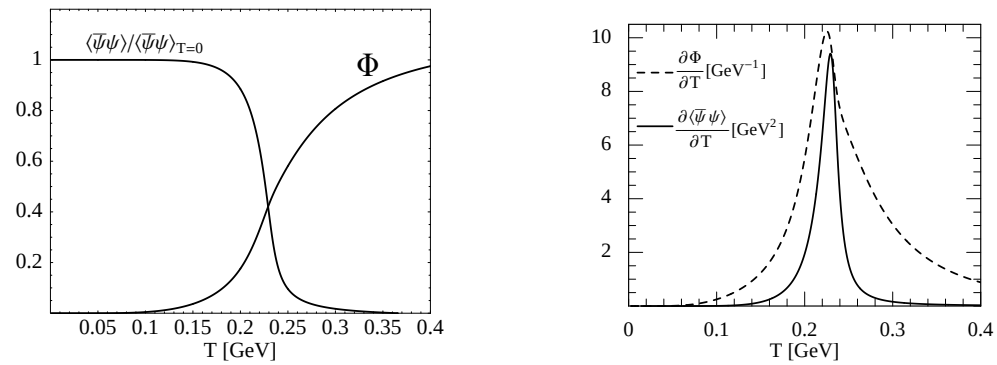

Figure 3: Left: scaled chiral condensate $\langle\overline{q}q\rangle$ and Polyakov loop $\Phi(T)$ as functions of temperature at zero chemical potential. Right: plots of $\partial\langle\overline{\psi}\psi\rangle/\partial T$ and $\partial\Phi/\partial T$.

where the modified Fermi – Dirac distribution functions f_Φ^+ and f_Φ^- have been introduced[4] (with the usual notation $\beta = 1/T$):

$$f_\Phi^+(E_p) = \frac{\left(\Phi + 2\overline{\Phi}e^{-\beta(E_p-\mu)}\right)e^{-\beta(E_p-\mu)} + e^{-3\beta(E_p-\mu)}}{1 + 3\left(\Phi + \overline{\Phi}e^{-\beta(E_p-\mu)}\right)e^{-\beta(E_p-\mu)} + e^{-3\beta(E_p-\mu)}} \tag{9}$$

$$f_\Phi^-(E_p) = \frac{\left(\overline{\Phi} + 2\Phi e^{-\beta(E_p+\mu)}\right)e^{-\beta(E_p+\mu)} + e^{-3\beta(E_p+\mu)}}{1 + 3\left(\Phi + \overline{\Phi}e^{-\beta(E_p+\mu)}\right)e^{-\beta(E_p+\mu)} + e^{-3\beta(E_p+\mu)}}, \tag{10}$$

On Fig. 3 the order parameters for chiral and deconfining transitions are shown together for $\mu = 0$. One observes that both transitions occurs as crossovers as it is expected: the chiral symmetry is explicitly broken *via* the bare quark mass term and the $\mathbb{Z}_3$ symmetry is exact only when quarks are static. A most striking fact is that both crossovers occur at almost the same temperature, a prediction of lattice calculations that this model is able to reproduce with very simple ingredients.

A detailed discussion of the results in mean field approximation can be found in the recent literature; for the purpose of this article, we only briefly discuss the result obtained in [4] for the pressure and the net quark number density, defined by the equation

$$\frac{n_q(T,\mu)}{T^3} = -\frac{1}{T^3}\frac{\partial\Omega(T,\mu)}{\partial\mu}, \tag{11}$$

that we display in Fig. 4. One can see that the NJL model (corresponding to the $\Phi \to 1$ limit of PNJL) badly fails in reproducing the lattice findings, while the PNJL results provide a good approximation for them.

The pressure in the NJL model (Fig. 4, left) is far from saturating the Stefan-Boltzmann (SB) limit (ideal gas limit) due to the lack of gluonic degrees of freedom.

[4]They have been explicitly derived and their role described in [5].

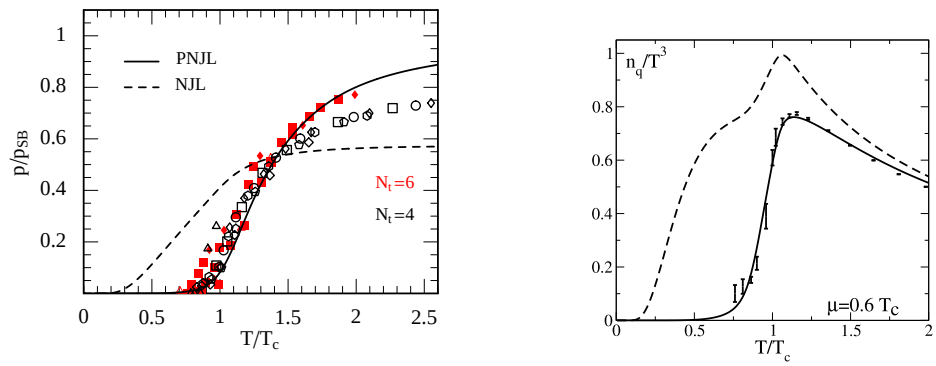

Figure 4: From C. Ratti *et al*, Ref. [4]. Left: Pressure over Stefan-Boltzmann constant as a function of the temperature, at zero chemical potential: PNJL (line), NJL (dashed line) and lattice results (A. Ali Khan *et al.*, Ref. [7]). Right: Quark number density: PNJL (line), NJL (dashed line) at $\mu = 0.6T_c$.

One cannot strictly speak of gluonic degrees of freedom in the PNJL model since there is no dynamical term for the gauge field; anyway the effective potential $\mathcal{U}$ (that reproduces well the pure gauge pressure) allows the SB limit to be reached and a very good agreement with the lattice results.

Another effect of the Polyakov loop can be seen by inspecting how quarks are affected by their propagation into the static field A_4. One realizes that, at a given value of T and μ, the NJL model always overestimates the density (Fig. 4, right), even if the two models merge for large temperatures (when in PNJL $\Phi \to 1$). On the other hand in the PNJL model below T_c (when $\Phi, \overline{\Phi} \to 0$) one can see from Eqs. (6) and (7) that contributions to the pressure coming from one and two (anti-)quarks are frozen, due to their coupling with Φ and $\overline{\Phi}$, while three (anti-)quark contributions are not suppressed. This implies that, at fixed values of T and μ, the PNJL value for n_q is much lower than in the NJL case. In fact all the possible contributions to the latter turn out to be somehow suppressed: the one- and two-quark contributions because of $\Phi, \overline{\Phi} \to 0$, while the thermal excitation of three quark has a negligible Boltzmann factor. One would be tempted to identify these clusters of three dressed (anti-)quarks with precursors of (anti-)baryons but no binding for these structures is provided by the model. In any case it is encouraging that coupling the NJL Lagrangian (whose parameters are chosen to reproduce zero temperature properties) with the Polyakov loop field (described by a pure gauge effective potential) leads to results pointing into the right direction.

We conclude this Section by stressing that Eqs. (9) and (10) allow to straightforwardly generalize NJL results to the PNJL case [5] by replacing the usual Fermi – Dirac occupation numbers by the modified ones.

2 Phase diagram and critical behavior

We now study thermodynamic properties of strongly interacting matter using the NJL and PNJL model (following what have been done in [8]). We focus our attention on the critical end point (CEP) and the physics near it, through the behavior of the baryon number susceptibility and the specific heat (for a detailed discussion, see [8]). We also study these models in the chiral limit where the CEP becomes a tricritical point (TCP).

The baryon number susceptibility χ_q and the specific heat C are the response of the baryon number density $\rho_q(T,\mu)$ and the entropy $S(T,\mu)$ to an infinitesimal variation of the quark chemical potential μ and temperature, given respectively by:

$$\chi_q = \left(\frac{\partial \rho_q}{\partial \mu}\right)_T \qquad \text{and} \qquad C = \frac{T}{V}\left(\frac{\partial S}{\partial T}\right)_\mu . \tag{12}$$

2.1 Phase diagram and critical region

A common feature shared by NJL and PNJL models is that the thermodynamic potential may have two degenerate minima at which two phases have equal pressure and chemical potential and can coexist according to the Gibbs criterion. In fact, this pattern is characteristic of a first order phase transition: the two minima correspond, respectively, to the phases of broken and restored symmetry. The quark condensate can be identified with the order parameter whose values allow to distinguish the two coexisting phases.

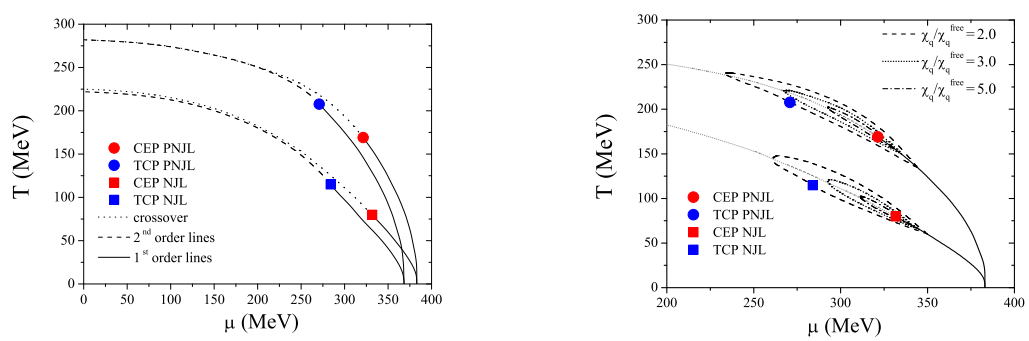

Figure 5: Left panel: the phase diagram in the PNJL and NJL models. Right panel: the size of the critical region is plotted for $\chi_q/\chi_q^{free} = 2, 3, 5$.

On Fig. 5 starting from zero temperature and increasing the chemical potential, such a first order phase transition is found. As the temperature increases, the first order transition persists up to the CEP. At the CEP the chiral transition becomes

	T^{CEP}	μ^{CEP}	density	T^{TCP}	μ^{TCP}
PNJL	169.11 MeV	321.32 MeV	2.76 ρ_0	207.66 MeV	270.80 MeV
NJL	79.92 MeV	331.72 MeV	2.95 ρ_0	112.08 MeV	286.05 MeV

Table 1: Position of the CEP (TCP in the chiral limit) for the NJL and PNJL model.

of second order. For temperatures above the CEP the thermodynamic potential has only one minimum and the transition is washed out: a smooth crossover takes place. We also verified that, in the chiral limit, the transition is of second order at $\mu = 0$ and, as μ increases, the line of second order phase transition will end in a first order line at the TCP.

While from a qualitative point of view the results of both models are similar, they differ quantitatively in two aspects (see Tab. 1): in PNJL, the CEP (TCP) are pushed to higher values of the temperature (closer to lattice results [9]) and the size of the critical region (that may be relevant for future searches of the CEP in heavy ion collisions) is larger (see Fig. 5). To estimate the critical region around the CEP we calculate the dimensionless ratio χ_q/χ_q^{free}, where χ_q^{free} is obtained taking the chiral limit $m_0 = 0$. The right panel of Fig. 5 shows a contour plot for three fixed ratios ($\chi_q/\chi_q^{free} = 2.0, 3.0, 5.0$) in the phase diagram around the CEP where we notice an elongation of the region where χ_q is enhanced, in the direction parallel to the first-order transition line. We also observe that the critical region is heavily stretched in the direction of the crossover transition line compared to the NJL results. It means that the divergence of the correlation length at the CEP affects the phase diagram quite far from it. As seen in [5] (Fig. 7), one of the main effects of the Polyakov loop is to shorten the temperature range where the crossover occurs (at $\mu = 0$ the crossover occurs within a range of 150 MeV for the NJL model and within 115 MeV for the PNJL one), thus resulting in higher baryonic susceptibilities even far from the CEP. The crossover taking place in a smaller temperature range can be interpreted as a crossover transition closer to a second order one than in the NJL model.

With this indication of the important role of the entanglement of the chiral and the Polyakov loop dynamics on the critical behavior of the QCD phase diagram, it is mandatory to investigate the behavior of χ_q and C in the vicinity of the CEP and their critical exponents, in the framework of the PNJL model. For comparison purposes with the NJL model and the universality/mean-field predictions, the critical exponents at the CEP and the TCP will be calculated in the next paragraph.

2.2 Critical exponents

The critical exponents (denoted ϵ and α for χ_q and C, respectively) are determined by following two directions, magnetic-field–like and temperature-like, in the $(T - \mu)$-

plane near the CEP or TCP (results are summarized in Tab. 2).

For the baryon number susceptibility we found that all the results are in agreement with the mean-field theory predictions ($\epsilon \simeq 2/3$ and in the chiral limit $\gamma_q \simeq 1/2$). We also study the baryon number susceptibility from higher μ towards the critical value μ^{CEP}. Our result shows that $\epsilon' = 0.69 \pm 0.02 \approx \epsilon$. This means that the size of the region we observe is approximately the same independently of the direction we choose for the path parallel to the μ-axis (see Fig. 6, left panel).

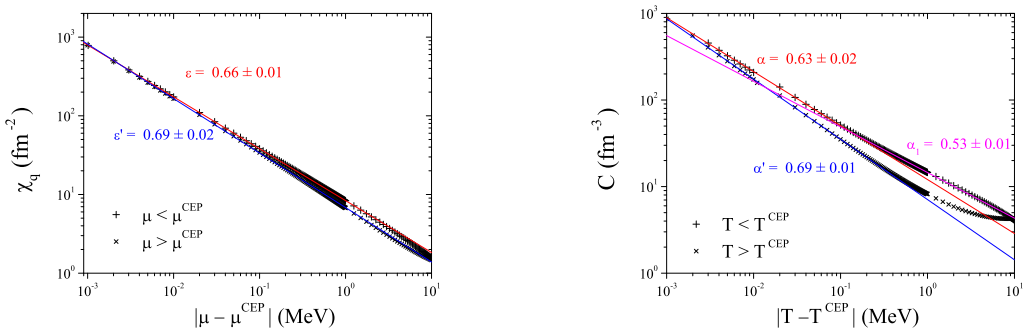

Figure 6: Left panel: baryon number susceptibility in PNJL as a function of $|\mu - \mu^{CEP}|$ at the fixed $T = T^{CEP}$. Right panel: specific heat as a function of $|T - T^{CEP}|$ at the fixed $\mu = \mu^{CEP}$.

Now, paying attention to the specific heat around the CEP, we have used a path parallel to the T-axis in the (T, μ)-plane from lower (higher) T towards the critical point at fixed μ^{CEP}. In Fig. 6 (right panel) we plot C as a function of T close to the CEP in a logarithmic scale. We see that for the region $T < T^{CEP}$ we have $\alpha = 0.63 \pm 0.02$. Contrarily to what happens in the NJL model (see Tab. 2 and Ref. [8]), this value of α is closer to the one suggested by universality arguments in [10]. We also observe, as in in Ref. [8], that in PNJL (NJL) model for the region $T < T^{CEP}$, the slope of data points changes for values of $|T - T^{CEP}|$ around 0.3 MeV. We have fitted the data which have a linear behavior for several orders of magnitude for $|T - T^{CEP}| < 0.3$ MeV and $|T - T^{CEP}| > 0.3$ MeV separately. We obtained, respectively, the critical exponent $\alpha = 0.63 \pm 0.02$ (NJL: $\alpha = 0.59 \pm 0.01$) and $\alpha_1 = 0.53 \pm 0.01$ (NJL: $\alpha_1 = 0.45 \pm 0.01$). As pointed out in [10], this change of the exponent can be interpreted as a crossover of different universality classes, with the CEP being affected by the TCP. In both models, the influence of the TCP is stronger in the specific heat rather than in the baryon number susceptibility: the closest distances between the TCP and the CEP in both phase diagrams occur in the T-direction ($T^{TCP} - T^{CEP} < \mu^{CEP} - \mu^{TCP}$). When the CEP is approached from above the trivial exponent $\alpha' = 0.69$ (for both models) is obtained. Finally for what concerns the specific heat around the TCP, as shown in Tab. 2, we find a nontrivial

critical exponent $\alpha = 0.40 \pm 0.02$ only for the NJL model while for the PNJL model we recover the universal behavior $\alpha = 0.50 \pm 0.01$.

Quantity	exponent/path	PNJL	NJL	Universality
χ_q	ϵ / $\rightarrow\bullet$	0.66 ± 0.01	0.66 ± 0.01	2/3
	ϵ' / $\bullet\leftarrow$	0.69 ± 0.02	0.66 ± 0.01	2/3
	γ_q / $\rightarrow\bullet$	0.51 ± 0.01	0.51 ± 0.01	1/2
C	α / $\bullet$	$\alpha = 0.63 \pm 0.02$	0.59 ± 0.01	2/3
		$\alpha_1 = 0.53 \pm 0.01$	0.45 ± 0.01	—
	α'/ $\downarrow$ $\bullet$	0.69 ± 0.01	0.69 ± 0.01	2/3
	α / $\bullet$ $\uparrow$	0.50 ± 0.01	0.40 ± 0.02	1/2

Table 2: Critical exponents: arrow $\rightarrow$ ($\uparrow$) indicates the path in the $\mu\,(T)-$ direction.

2.3 Isentropic lines

Finally we report on a preliminary result obtained by P. Costa, C. A de Sousa, M. C. Ruivo and H.H.. The isentropic lines play a very important role in the understanding of thermodynamic properties of matter created in relativistic heavy ion collisions. Some studies predict that in a region around the CEP the properties of matter are only slowly modified as the collision energy is changed as a consequence of the attractor character of the CEP [10].

We have used another set of parameters to do this calculation: $\Lambda = 590$ MeV, $G_1 = 2.435/\Lambda^2$ GeV^{-2} and $m_0 = 5.5$ MeV ($|\langle\overline{q}q\rangle|^{1/3} = 241.5$ MeV , $f_\pi = 92.6$ MeV, $m_\pi = 140.2$ MeV, $m = 6.0$ MeV). Indeed, with this set at $T = 0$, all isentropic trajectories directly terminate at the first order transition line (see Fig. 7), without reheating in the mixed phase as seen in the "zigzag" shape of [11]. This is a very important point since in the limit $T \rightarrow 0$, it is verified that $s \rightarrow 0$ and $\rho_q \rightarrow 0$, as it should be (third law of thermodynamics or Nernst principle) ; this was not verified with the previous set of parameters. Our convenient choice of the model parameters allows a first order phase transition that is stronger than in other treatments of the NJL (PNJL) model; this is crucial to obtain these two important results: it fulfills the criterion of stability of the quark droplets [2], and, in addition, it is also crucial to the satisfaction of the third law of thermodynamics in the limit $T \rightarrow 0$.

On Fig. 7 we see that the isentropic lines ($s/\rho = 1, ..., 6$) come from the region of symmetry partially restored and attain directly the phase transition, going along the phase transition as T decreases until it reaches $T = 0$.

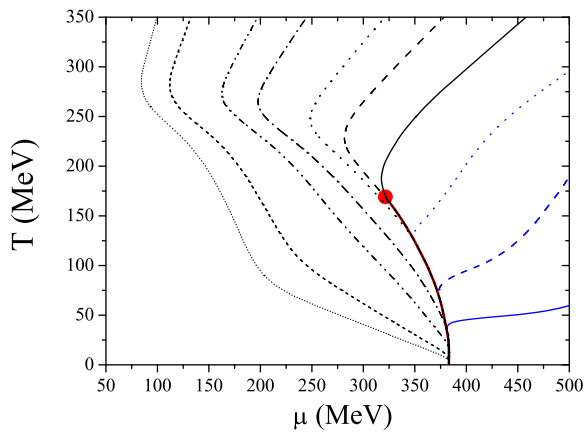

Figure 7: Isentropic trajectories in the $T-\mu$ plane using the parameter Set A. The following values of the entropy per baryon number have been considered: $s/\rho =$ 1, 2, 3, 4, 5, 6, 8, 10, 15, 20 (from left to right).

In the crossover region the behavior of the isentropic lines is qualitatively similar to the one obtained in lattice calculations or in some models [11]. It is interesting to note that we can see a slight "focusing" effect like it can be seen in some of these works.

3 Conclusions

The Polyakov loop extended Nambu–Jona-Lasinio model has proved to be particularly successful in reproducing two flavor QCD thermodynamics as obtained in lattice calculations [4]: the coupling of quarks to the Polyakov loop produces a statistical suppression of the one- and two-quark contributions to the thermodynamics, thus remarkably improving the NJL model results at low temperatures.

The successful comparison with lattice results shows that the model calculation provides a convenient tool to obtain information for systems from zero to non zero chemical potential which is of particular importance for the knowledge of the equation of state of hot matter, relevant for the upcoming LHC experiments at CERN, and for dense matter, relevant for the CBM one at FAIR.

We investigated its phase structure at finite T and μ. Evaluating the thermodynamical potential we find the critical curves on the $T-\mu$ plane. Working out of the chiral limit, a CEP which separates the first and the crossover line is found.

The observation of differential observables like the entropy and the heat capacity and their temperature and density behavior serve as important probes which, to-

gether with lattice data, are important for phenomenology of heavy ion collisions and cosmology.

References

[1] Y. Nambu, G. Jona-Lasinio, Phys. Rev. **122**, 345 (1961) and Phys. Rev. **124**, 246 (1961) ; S. P. Klevansky, Rev. Mod. Phys. **64**, 649 (1992).

[2] M.Buballa, Phys. Rep. **407**, 205 (2005).

[3] P. N. Meisinger, M. C. Ogilvie, Phys. Lett. B **379**, 163 (1996); R.D. Pisarski Phys. Rev. **D62**, 111501 (2000); P. N. Meisinger, T. R. Miller, M. C. Ogilvie, Phys. Rev. D **65**, 034009 (2002); K. Fukushima, Phys. Lett. B **591**, 277 (2004); A. Mocsy, F. Sannino, K. Tuominen, Phys. Rev. Lett. **92** (2004) 182302.

[4] C. Ratti, M. A. Thaler, W. Weise, Phys. Rev. **D73**, 014019 (2006).

[5] H. Hansen, W.M. Alberico, A. Beraudo, A. Molinari, M. Nardi, C. Ratti, Phys. Rev. D **75**, 065004 (2007).

[6] Kenji Fukushima, Phys. Rev. D **77**, 114028 (2008) ; C. Sasaki, B. Friman, K. Redlich Phys. Rev. D **75**, 074013 (2007);S. Rößner, C. Ratti, W. Weise, Phys. Rev. D **75**, 034007 (2007).

[7] O. Kaczmarek, F. Karsch, P. Petreczky, F. Zantow, Phys. Lett. B **543**, 41 (2002); G. Boyd *et al.*, Nucl. Phys. B **469**, 419 (1996); A. Ali Khan *et al.* Phys. Rev. D **64**, 074510 (2001).

[8] P. Costa, C. A de Sousa, M. C. Ruivo, Yu. L. Kalinovsky, Phys. Letts. B **647**, 431 (2007); P. Costa, C. A. de Sousa, M. C. Ruivo, Phys. Rev. D **77**, 096001 (2008); P. Costa, C. A. de Sousa, M. C. Ruivo, H. Hansen, Europhys. Lett. **86**, 31001 (2009).

[9] F. Karsch, AIP Conf. Proc. **842** (2006) 20; Fodor, Katz, J. HEP. 0204 (2004).

[10] Y. Hatta, T. Ikeda, Phys. Rev. D **67**, 014028 (2003); B.-J. Schaefer, J. Wambach, Phys. Rev. D **75**, 085015 (2007); M. Stephanov, K. Rajagopal, E. Shuryak, Phys. Rev. Lett. **81**, 4816 (1998).

[11] P. R. Subramanian, H. Stocker, W. Greiner, Phys.Lett. B**173**, 468 (1986); S. Ejiri, F. Karsch,E. Laermann, C. Schmidt, Phys.Rev. D**73**, 054506 (2006); C. Nonaka, M. Asakawa, Phys.Rev. C**71**, 044904 (2005); T. Kahara, K. Tuominen, Phys.Rev. D**78**, 034015 (2008); K. Fukushima, Phys. Rev. D **79**, 074015 (2009).